Available online at www.sciencedirect.com
ScienceDirect
Journal of Power Sources 161 (2006) 550–559
JOURNAL OF POWER SOURCES
www.elsevier.com/locate/jpowsour

Poly-ether modified siloxanes as electrolyte additives for rechargeable lithium cells

Tsuyoshi Inose, Satoru Tada, Hideyuki Morimoto, Shin-ichi Tobishima *

Department of Material Science, Faculty of Engineering, Gunma University, Kiryu, Gunma 376-8515, Japan

Received 1 March 2006; received in revised form 16 March 2006; accepted 17 March 2006
Available online 30 May 2006

Abstract

Influence of four poly-ether modified siloxanes as electrolyte additives on charge–discharge cycling properties of lithium was examined. As siloxanes, diethylene glycol methyl-(3-dimethyl(trimethylsiloxy)silyl propyl)ether (sample A), diethylene glycol methyl-(3-dinethyl(trimethylsiloxy)silyl propyl)-2-methylpropyl ether (sample B), diethylene glycol methyl-(3-bis(trimethylsiloxy)silyl propyl)ether (sample C) and diethylene glycol-(3-methyl-bis(trimethylsiloxy)silyl-2-methylpropyl)ether (sample D) were investigated. As a base electrolyte solution, 1 M (M, mol L^{-1}) $LiPF_6$-ethylene carbonate (EC)/methylethyl carbonate (MEC) (mixing volume ratio = 3:7) was used. As the anodes, lithium metal, natural graphite carbon and silicon–SiO_2–carbon (Si–C) composite electrodes were used. Lithium cycling efficiencies of these three anodes improved and an impedance of anode/electrolyte interface decreased by adding poly-ether modified siloxanes. Graphite/$LiCoO_2$ and Si–C/$LiCoO_2$ cells exhibited better anode utilization and good cycling performance by using 1 M $LiPF_6$–EC/MEC + siloxane electrolytes. It was also found that thermal stability of the electrolyte solutions improved by adding siloxanes. Thermal decomposition temperature of 1 M $LiPF_6$–EC/MEC shifted to higher temperature by adding siloxanes. Amount of heat-output of graphite–lithium anodes with M $LiPF_6$–EC/MEC electrolyte solutions decreased and the temperature starting the heat-output shifted to higher temperature by adding siloxanes. Among siloxanes examined here, samples B and D exhibited much better performance.

Keywords: Lithium cell; Electrolyte; Siloxane; Cell safety; Carbon anode; Silicon anode

1. Introduction

Many of commercial lithium ion cells are composed of carbon anode and $LiCoO_2$ cathode with nonaqueous electrolyte solutions. Typical example of nonaqueous electrolyte solutions is $LiPF_6$–ethylene carbonate (EC)/methylethyl carbonate (MEC). The improvement of energy density of lithium ion cells has been required every year. However, now the capacity of carbon anodes is getting closer to the theoretical value (372 mA h g^{-1}). Then, new anode materials having higher energy density than carbon have been studied. Examples of these materials are lithium metal, various Si- and Sn-based compounds [1]. At this stage, the cycleability of these materials is not sufficient for commercial use. The choice of the electrolyte materials (solvents and solutes) is one of the most important factors for the charge–discharge cycling performance of lithium cells with various anodes.

Many researches on the electrolyte solutions have been carried out for improving lithium cycleability [2]. One of these researches is an addition of surfactants (surface active agents) to electrolyte solutions such as poly-ethyleneglycol dimethyl ethers [3]. The mechanism of lithium cycling efficiency enhancement by the addition of these compounds is explained as follows. These compounds are less reactive toward lithium and adsorbed on the lithium anode surface. This adsorption layer suppresses the lithium dendrite formation and the reduction of electrolyte solutions by lithium [3].

In this study, influence of poly-ether modified siloxanes as electrolyte additives on lithium cycling efficiency was examined. As siloxanes, diethylene glycol methyl-(3-dimethyl(trimethylsiloxy)silyl propyl)ether (sample A), diethylene glycol methyl-(3-dinethyl(trimethylsiloxy)silyl propyl)-2-methylpropyl ether (sample B), diethylene glycol methyl-(3-bis(trimethylsiloxy)silyl propyl)ether (sample C) and diethylene glycol-(3-methyl-

* Corresponding author. Tel.: +81 277 30 1382; fax: +81 277 30 1380.
E-mail address: tobi@chem.gunma-u.ac.jp (S.-i. Tobishima).

0378-7753/$ – see front matter © 2006 Elsevier B.V. All rights reserved.
doi:10.1016/j.jpowsour.2006.03.053

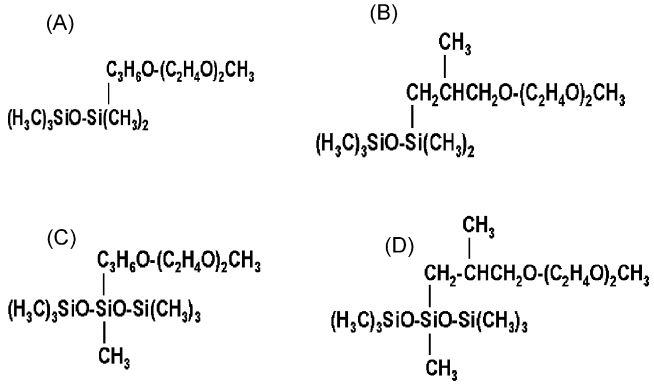

Fig. 1. Chemical structure of poly-ether modified siloxanes. Sample A, diethylene glycol methyl-(3-dimethyl(trimethylsiloxy)silyl propyl)ether; sample B, diethylene glycol methyl-(3-dinethyl(trimethylsiloxy)silyl propyl)-2-methylpropyl ether; sample C, diethylene glycol methyl-(3-bis(trimethylsiloxy)silyl propyl)ether and sample D, diethylene glycol-(3-methyl-bis(trimethylsiloxy)-silyl-2-methylpropyl)ether.

Table 1
Viscosities of siloxanes

Siloxanes	Kinematic viscosity at 20 °C ($\times 10^{-4}$ m^2 s^{-1})
Sample A	3.3
Sample B	3.7
Sample C	4.0
Sample D	4.3

bis(trimethylsiloxy)silyl-2-methylpropyl)ether (sample D) were investigated. As the base electrolyte solution, 1 M (M, mol L^{-1}) $LiPF_6$–EC/MEC (3:7 in volume mixing ratio) was used. As the anodes, lithium metal, natural graphite carbon and Si–SiO_2–carbon composite (Si–C) anodes were investigated. Fig. 1 shows the chemical structure of four siloxanes used in this work. Chemical bonding of Si–O is stronger and more stable than that of C–O. The siloxanes shown in Fig. 1 have ether groups as hydrophilic groups and they work as the surfactants. They are colorless and clear liquid at room temperature. Their kinematic viscosities are less than 5×10^{-4} m^2 s^{-1} at 20 °C (Table 1).

2. Experimental

2.1. Preparation of electrolyte solutions

Siloxanes were obtained from Shin-Etsu Chemical Co. Electrolyte solutions were prepared by mixing siloxanes and 1 M $LiPF_6$–EC/MEC (3:7 in volume ratio) (Tomiyama Pure Chemicals Co., Lithium Battery Grade). Before mixing, siloxanes were dried over molecular sieves 3A (Kanto Chemicals Co.). Water content of electrolyte solutions was less than 20 ppm as determined by the Karl-Fisher titration method. Hereafter, "EM" represents 1 M $LiPF_6$–EC/MEC (3:7).

2.2. Charge–discharge cycling tests of lithium anodes and $LiCoO_2$ cells

Cyclic voltammetry was performed, using a glass cylindrical test cell with a lithium metal sheet counter electrode (0.1 mm thickness) pressed on a Ni net (200 mesh, 15 mm length, 4 mm width, 0.05 mm thickness) and a Pt working electrode (4 mm length, 4 mm width and 0.05 mm thickness, 0.09 cm^2). Lithium charge–discharge cycling tests were carried out galvanostatically, using a coin cell (coin type 2032, diameter 20 mm in diameter, 3.2 mm in thickness) with a lithium metal sheet counter electrode (0.1 mm thickness, 15 mm diameter) and a stainless steel (SUS 316) cathode case of the coin cell as the working electrode. The charge–discharge cycling efficiency (Eff) was obtained from the ratio of the stripping charge (Q_s)/plating charge (Q_p) on the stainless steel electrode with a charge–discharge voltage range of −2.0 to 1.0 V. The charge–discharge current density (Ips) was 0.5 mA cm^{-2}. The Q_p had a constant value of 0.5 mA h cm^{-2}.

In cases of Si–SiO_2–carbon composite (Si–C) and natural graphite electrodes, the charge–discharge tests were carried out by the charge–discharge voltage cut-off (0 and 1.5 V versus Li/Li$^+$) with a constant current density of 0.5 mA cm^{-2} by using the 2032 coin cells. These cells have a lithium metal counter electrode and the working electrode of Si–C or graphite. Using the 2032 coin cells carried out the charge–discharge test of $LiCoO_2$/C and $LiCoO_2$/Si–C cells.

For these experiments, we prepared the printed carbon electrodes by coating a Ni sheet with a mixture of carbon powder (around 18 mg) and poly(vinylidene fluoride) (PVDF) (weight ratio of carbon:PVDF = 9:1) in *N*-methyl pyrolidinone (NMP). We then evacuated the solvent and dried the electrodes. The printed carbon electrodes are 15 mm in diameter and 0.15 mm in thickness. Natural graphite powder used here has an average particle size of 10.7 μm in diameter, a surface area of 10.3×10^3 m kg^{-1} and a density of 0.21 kg m^{-3}. The printed $LiCoO_2$ electrodes were prepared by coating an Al sheet with a mixture of carbon powder (around 18 mg) and poly(vinylidene fluoride) (PVDF) (weight ratio of carbon:PVDF = 9:1) in *N*-methyl pyrolidinone (NMP). We then evacuated the solvent and dried the electrodes.

The printed Si–C electrodes (15 mm in diameter and 0.15 mm in thickness) were prepared by similar method as natural carbon electrodes by using Si–C powder and polymer binder. Si–C material was prepared according to the papers [4–6] by methane–argon gas mixture-chemical vapor deposition (CVD) with 1100 °C heat treatment. Image of this final product of Si–C material is shown in Fig. 2. Fine silicon crystal was distributed in the SiO_2. The surface of the final product was covered with double layers composed of thin inside layer of SiC (silicon carbide) and thick outside layer of carbon.

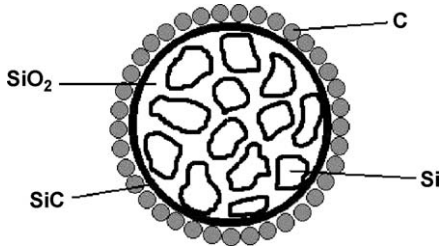

Fig. 2. Image of Si–SiO_2–carbon composite (Si–C).

All the electrochemical measurements were carried out at 25 °C.

2.3. Thermal stability tests of electrolyte solutions

Thermal behavior of electrolyte solutions alone and that of the electrolyte solutions toward C_6Li_x were evaluated with a differential scanning calorimeter (DSC, Rigaku Co., model TAS-100) and a crimp-sealed stainless steel pan. The DSC sample of 3 μl of electrolyte was used for the thermal stability tests of electrolyte solutions. In the thermal stability tests of the electrolyte solutions toward C_6Li_x ($x = 0.97$), the DSC sample was composed of about 7 mg of carbon and 3 μl of electrolyte. All the DSC experiments were carried out at a heating rate of 10 °C min^{-1} from room temperature to 450 °C.

3. Results and discussion

3.1. Charge–discharge cycling properties of lithium metal anodes in the electrolyte solutions with siloxanes

Cyclic voltammetry (cv) of lithium metal (Li) in EM + polyether modified siloxanes was carried out by using a glass cell consisted of Li counter and Pt working electrodes. Fig. 3 shows the cv results of Li at first cycle in EM alone and EM + siloxanes (sample D). The following three results were obtained: (i) lithium was able to be discharged and charged in EM + siloxanes; (ii) Li charge–discharge capacities in EM + siloxanes were larger than that in EM alone and (iii) Li charge–discharge capacity depended on the addition amounts of siloxanes. The Li discharge capacities was higher in the order of addition amounts of siloxanes (sample D) of 10 > 20 > 30 > 40 vol.% > 0% (EM alone). Fig. 4 shows the cv results of Li at 50th cycle in EM alone. In EM alone, charge–discharge capacity of Li considerably decreased after 50 cycles in comparison with that at first cycle. However, the charge–discharge capacity of Li was approximately constant after 50 cycles in EM with siloxanes (Fig. 5). Deterioration of lithium cycling behavior with an increase in cycle number became small by addition of siloxanes. So, better lithium cycleability in EM + siloxanes than that in EM alone was observed from these cv results.

Next, using a coin cell consisted of Li anode and SUS cathode carried out charge–discharge cycling tests of lithium. Charging capacity was 0.5 mA h cm^{-2}. Fig. 6 shows charge–discharge cycling test results of lithium metal anodes in EM + siloxanes

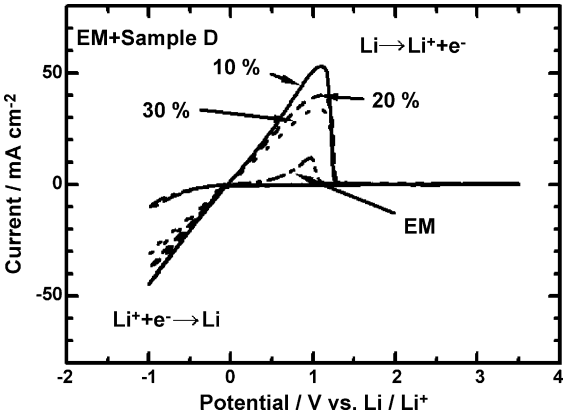

Fig. 3. Cyclic voltamgram of lithium in EM + siloxane (sample D). Pt working electrode; scanning rate, 100 mV cm^{-2}; −1.0 to 3.5 V vs. Li/Li^+.

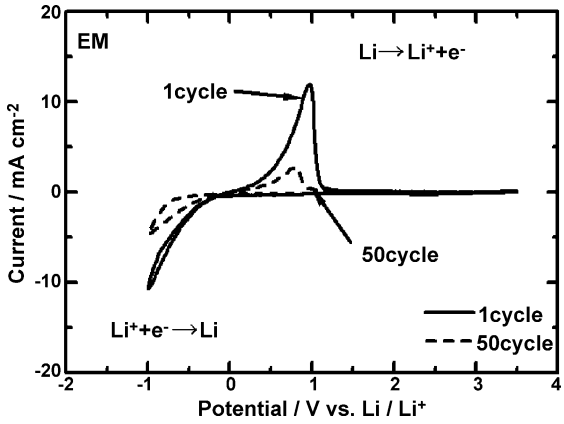

Fig. 4. Cyclic voltamgram of lithium in EM. Pt working electrode; scanning rate, 100 mV cm^{-2}; −1.0 to 3.5 V vs. Li/Li^+.

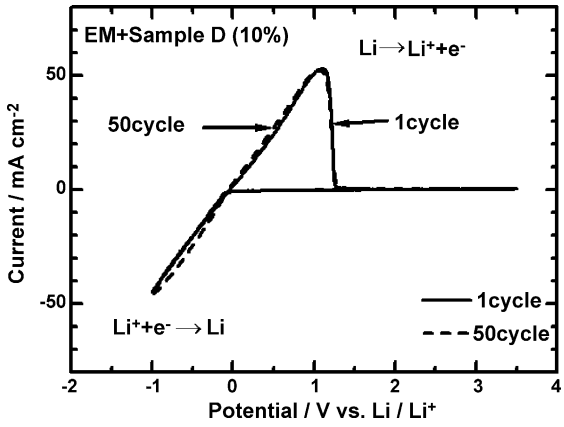

Fig. 5. Cyclic voltamgram of lithium in EM + siloxane (sample D, 10 vol.%). Pt working electrode; scanning rate, 100 mV cm^{-2}; −1.0 to 3.5 V vs. Li/Li^+.

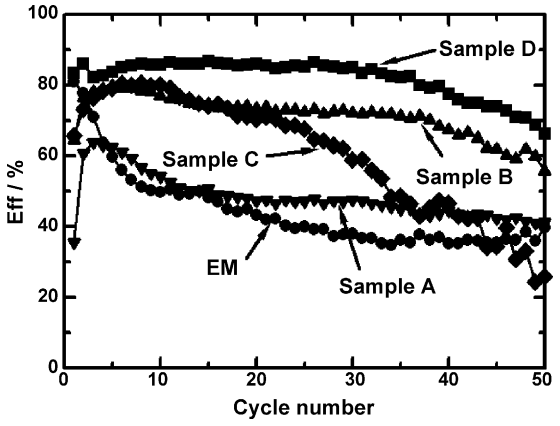

Fig. 6. Charge–discharge cycling tests results of lithium in EM + siloxanes (10 vol.%). SUS working electrode; Ips, 0.5 mA cm^{-2}; Q_p, 0.5 mA h cm^{-2}; charge–discharge cut-off voltages, −2.0 and 1.0 V vs. Li/Li^+.

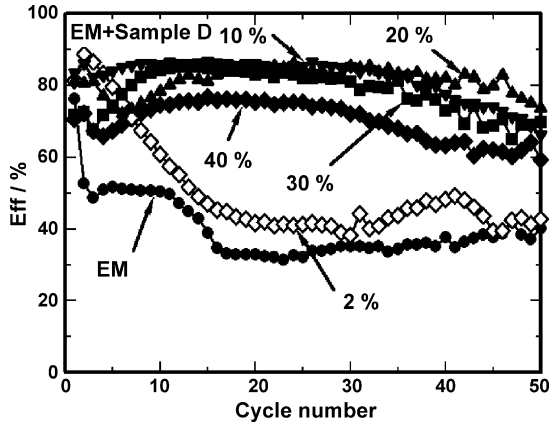

Fig. 7. Charge–discharge cycling tests results of lithium in EM + siloxane (sample D). SUS working electrode; Ips, 0.5 mA cm^{-2}; Q_p, 0.5 mA h cm^{-2}; charge–discharge cut-off voltages, −2.0 and 1.0 V vs. Li/Li$^+$.

(10 vol.%). Lithium cycling efficiencies (Eff) in EM + siloxanes were higher than that in EM alone. Average lithium cycling efficiencies from first to 50th cycle (Eff_{Av50}) was high in the order of sample B > sample D > sample C > sample A > EM. Among four siloxanes, the samples B and D exhibited much better Eff values. Then, influence of addition amounts of samples B and D on the Eff was examined. These results are shown in Fig. 7 (sample D) and Fig. 8 (sample B). The average Eff value from first to 50th cycle exhibited the maximum value at 10 vol.% additions for sample D and at 20 vol.% additions for sample B, respectively.

From the charge–discharge test results, it was found that the addition of siloxanes was effective for the improvement of cycling efficiency of lithium metal anodes.

In organic electrolyte solutions, the surface of lithium is covered with thin film after charge–discharge cycling [7]. This surface film is formed by the reduction of electrolyte solution by lithium. This film is generally known as the SEI (solid–electrolyte interface) [8]. The SEI is consisted of several chemical compounds such as alkyl lithium carbonate [7]. During charge and discharge, lithium ion must diffuse in the SEI. In many cases, this diffusion process is considered to be a rate-determining step for electrochemical reaction. To investigate

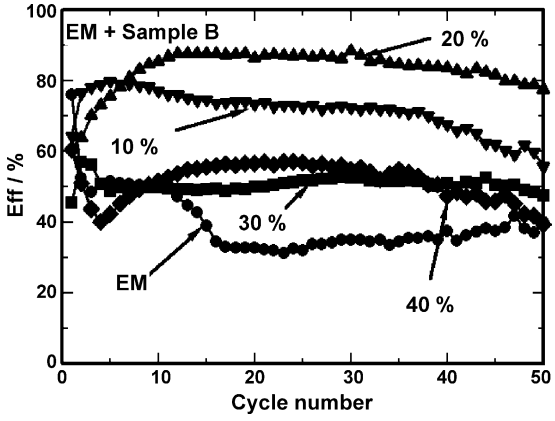

Fig. 8. Charge–discharge cycling tests results of lithium in EM + siloxane (sample B). SUS working electrode; Ips, 0.5 mA cm^{-2}; Q_p, 0.5 mAh cm^{-2}; charge–discharge cut-off voltages, −2.0 and 1.0 V vs. Li/Li$^+$.

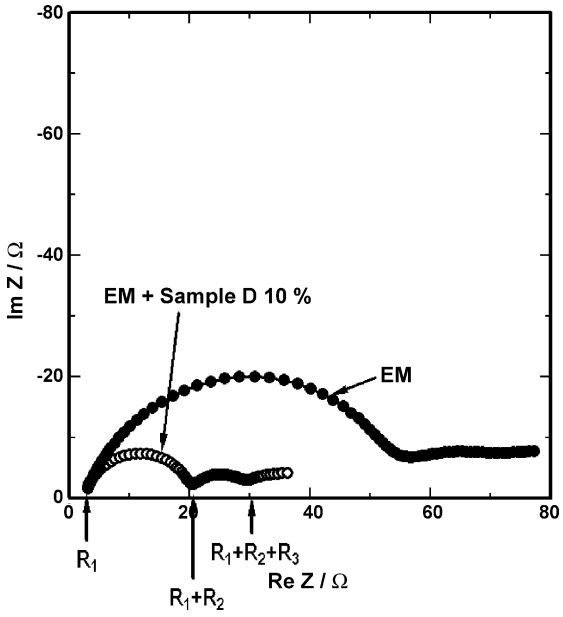

Fig. 9. Cole–Cole plot of Li/electrolyte interface, Li/Li cells, EM + sample D (10 vol.%) after first charge at 25 °C. Ips, 0.5 mA cm^{-2}; Q_p, 0.5 mA h cm^{-2}; charge–discharge cut-off voltages, −2.0 and 1.0 V vs. Li/Li$^+$.

the charge–discharge behavior of Li in EM + siloxanes in more detail, the a.c. impedance measurements of lithium/electrolyte interface were carried out by using Li/SUS coin cells. Before a.c. measurements, lithium was electrochemically plated on the SUS cathodes. Namely, the impedance measurements were carried out for the cells of Li/Li plated on SUS. Fig. 9 shows the Cole–Cole plot of Li/Li cells after first charge (plating Li on SUS). In Fig. 9, R_1 corresponds to the impedance of electrolyte solution. R_2 and R_3 correspond to the impedance of the interface between Li and the electrolyte solution, i.e., between SEI and electrolyte solution. Two components of impedance (R_2 and R_3) are also observed in EM alone. Two components of impedance may arise from the double layer structure of SEI, e.g., layers of organic compounds such as lithium alkyl carbonate and inorganic compounds such as LiF [7]. After first charge, an impedance of the electrolyte/Li interface in EM + sample D (10 vol.%) was smaller than that in EM alone. This result suggests that the impedance of the surface film or layer of lithium in EM + siloxanes is smaller than that in EM alone. Figs. 10 and 11 show a dependency of the impedance on temperature. With an increase in temperature, the impedance both in EM and in EM + siloxanes decreased. Between 25 and 70 °C, the impedance values in EM + siloxanes were lower than those in EM alone. The degree of the decrease in the impedance in EM + siloxanes was similar to that in EM alone.

To investigate the reactivity between Li and the electrolyte solutions, linear potential sweep measurements in the cathodic direction were carried out by using Li/SUS coin cells (Fig. 12). In EM alone, the reduction (cathodic reaction) shoulder was observed before Li deposition around −0.15 V. This shoulder corresponds to the reduction of EM. In EM + siloxane (sample D), the cathodic current became smaller. With an increase in the amounts of siloxane, this cathodic current decreased more. So,

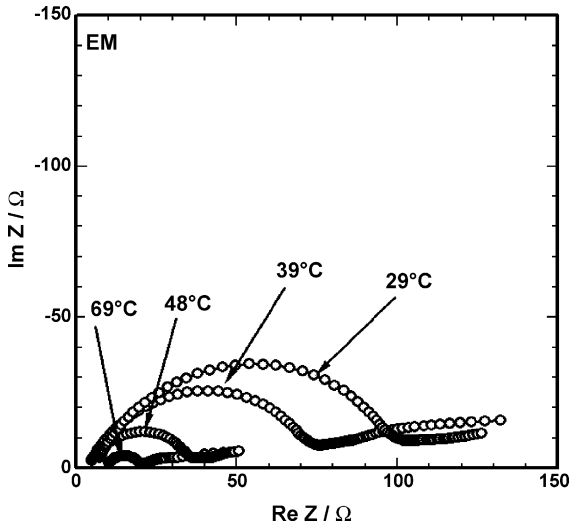

Fig. 10. Cole–Cole plot of Li/electrolyte interface, Li/Li cells, EM after first charge.

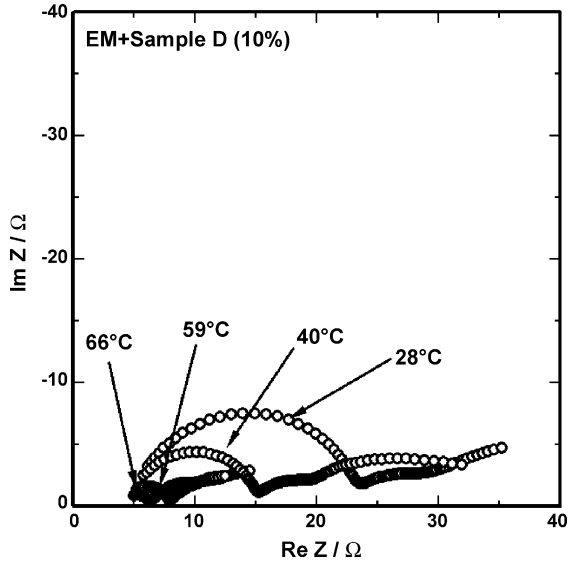

Fig. 11. Cole–Cole plot of Li/electrolyte interface, Li/Li cells, EM + sample D (10 vol.%) after first charge.

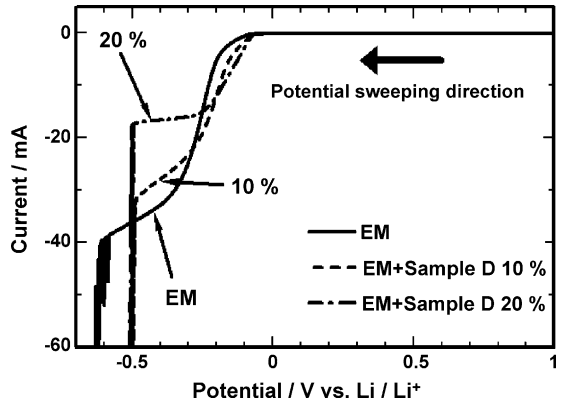

Fig. 12. Linear potential sweep results of EM + sample D. Scanning rate, 1 mV s^{-1}; sweeping from 3.0 to −1.0 V vs. Li/Li^+.

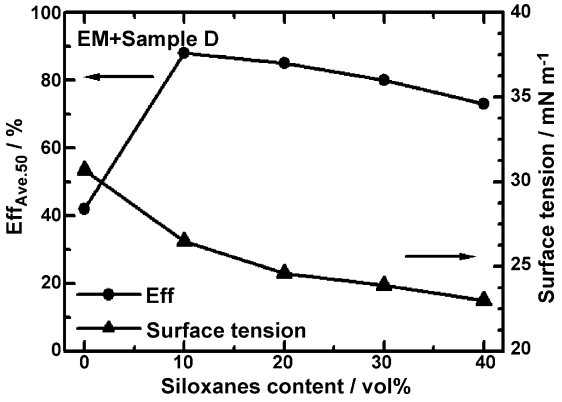

Fig. 13. Relationship between surface tension and average lithium cycling efficiency (Eff_{Av50}), EM + sample D.

the addition of siloxane is effective on suppressing the electrolyte reduction.

As mentioned above, siloxanes are effective on suppressing reactivity of electrolyte solution toward lithium. However, another possible effect of siloxanes on charge–discharge behavior of lithium should be noted here. Siloxanes are surfactants. Then, simple adsorption of siloxanes on Li electrode may occur. This phenomenon makes the wetting ability of the electrolytes for the anodes improve by a decrease in surface tension. When this phenomenon occurs, the active electrode surface area increases and electrode utilization improves. Therefore, one possible reason for the Eff enhancement by adding siloxanes is the improvement of wetting ability of the electrolyte for electrode. Figs. 13 and 14 show the relation between the surface tension and the addition amounts of siloxane. There is no distinct relation between the surface tension and Eff. The Eff maxima appear before the cmc (critical micelle concentration). Large amounts of siloxane addition such as 40 vol.% do not reach cmc yet. Because the surface tension does not reach constant value yet. So, the main reason for the Eff enhancement by adding siloxanes is not the improvement of the wetting ability of electrolyte solutions for lithium anode, though the wetting ability enhancement may be helpful for the Eff improvement.

Summarizing the results of lithium cycling efficiency measurements by cv and coin cells, impedance measurements, elec-

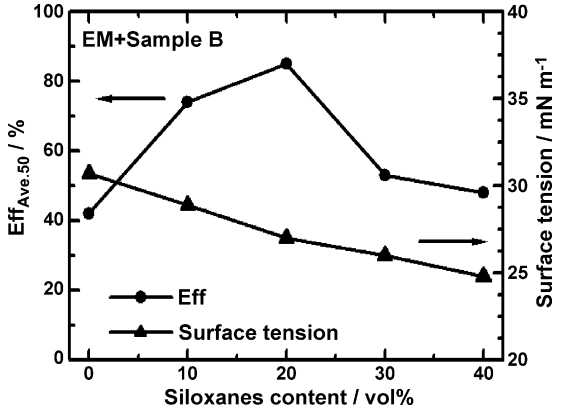

Fig. 14. Relationship between surface tension and average lithium cycling efficiency (Eff_{Av50}), EM + sample B.

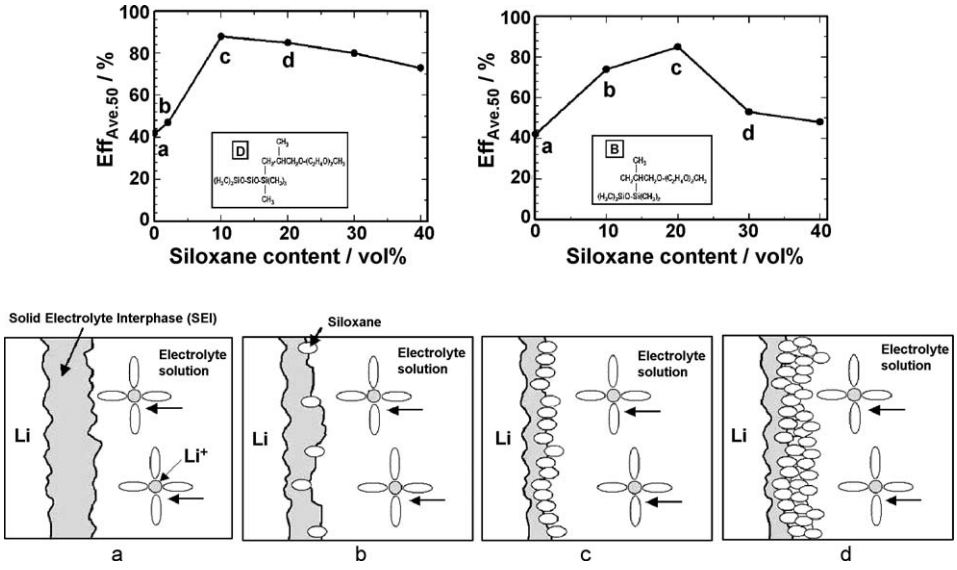

Fig. 15. Proposed mechanism for change in lithium cycling efficiency in EM + siloxanes.

trolyte reduction behavior and surface tension, the following mechanism may be proposed for the improvement of lithium cycling efficiency by addition of siloxanes. Fig. 15 shows the proposed models for the Eff enhancement by adding siloxanes. Just after charging (lithium deposition), freshly deposited lithium is chemically active. On the lithium surface, EM is chemically reduced by lithium and produces the surface film. The reduction products were reported to be solid compounds and gas compounds [7]. The solid compounds remained on the lithium produce the SEI. Fig. 15a – by no addition of siloxane, the surface film is composed of reduction products of EM; Fig. 15b – by the small addition of siloxane, the surface film is mainly composed of reduction products of EM. Small amounts of siloxane is involved in the SEI or it adsorbs on the SEI surface. Siloxanes are less reactive than EM; Fig. 15(c) – by the medium amounts of siloxane (10–20 vol.%), the surface film is thin and is composed of both the reduction product of EM and siloxane; Fig. 15(d) – by adding larger amounts of siloxane, the excess and thick siloxane layer exists around the lithium electrode. This excess siloxane could be resistive for the smooth charge–discharge of lithium (lithium ion diffusion). Then, the Eff improves by adding siloxanes and shows the maximum value against the addition amounts of siloxanes.

3.2. Charge–discharge cycling properties of lithium in graphite anodes in electrolyte solutions with siloxanes

Fig. 16 shows the charge–discharge cycling test results of natural graphite electrodes in EM + siloxanes (samples B and D) by using Li/graphite coin cells. Discharge capacity density (mA h g^{-1}) in *y*-axis of Fig. 17 is calculated based on graphite active material weight. Discharge capacity is the capacity of the lithium deintercalated from graphite electrodes. Both discharge capacity densities and the cycle life in EM + siloxanes were better than those in EM alone.

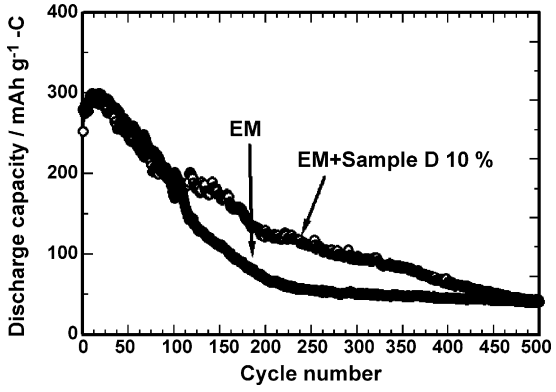

Fig. 16. Charge–discharge cycling tests results of graphite/Li cells with EM + siloxane (sample D, 10 vol.%). Ips, 0.5 mA cm^{-2}; charge–discharge cut-off voltages, 0 and 1.5 V.

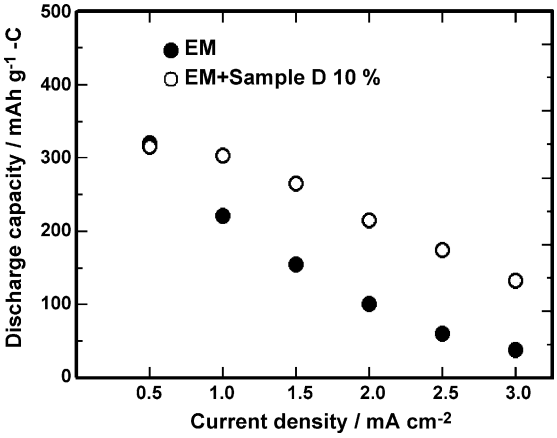

Fig. 17. Rate capability of graphite/Li cells with EM + siloxane (sample D, 10 vol.%). Charge–discharge cut-off voltages, 0 and 1.5 V vs. Li/Li^+.

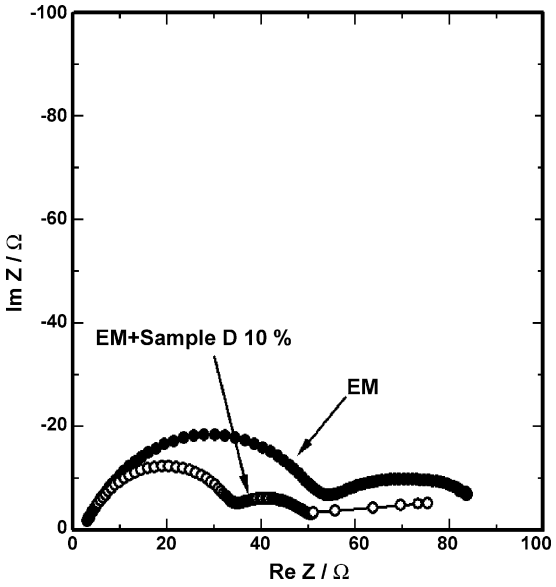

Fig. 18. Cole–Cole plot of graphite(Li)/electrolyte interface, graphite/Li cells, EM + sample D (10 vol.%) at 25 °C. Ips, 0.5 mA cm^{-2}; charge–discharge cut-off voltages, 0 and 1.5 V vs. Li/Li^+.

Fig. 18 shows the impedance of the interface between graphite electrode and electrolyte solutions. The impedance in EM + siloxane (sample D) was smaller than that in EM alone. Fig. 22 shows the discharge-rate capability of graphite electrodes. The rate capability in EM + siloxanes was better than that in EM alone. The discharge-rate determining step may be the diffusion of lithium ions through the SEI of graphite electrodes.

3.3. Charge–discharge cycling properties of lithium in Si–C anodes in the electrolyte solutions with siloxanes

Fig. 19 shows the charge–discharge cycling test results of Si–SiO_2–carbon composite (Si–C) electrodes in EM + siloxanes (samples B and D) by using Li/Si–C coin cells. Discharge capacity density (mA h g^{-1}) in *y*-axis of Fig. 19 is calculated based on the Si–C active material weight. Discharge capacity is the capacity of the lithium deintercalated from Si–C electrodes. Both

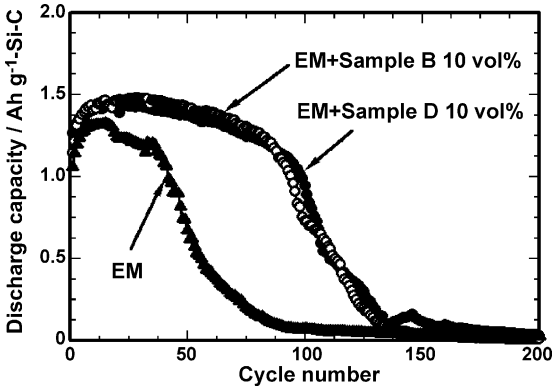

Fig. 19. Charge–discharge cycling tests results of Si–C/Li cells with EM + siloxanes (10 vol.%). Ips, 0.5 mA cm^{-2}; charge–discharge cut-off voltages, 0 and 1.5 V vs. Li/Li^+.

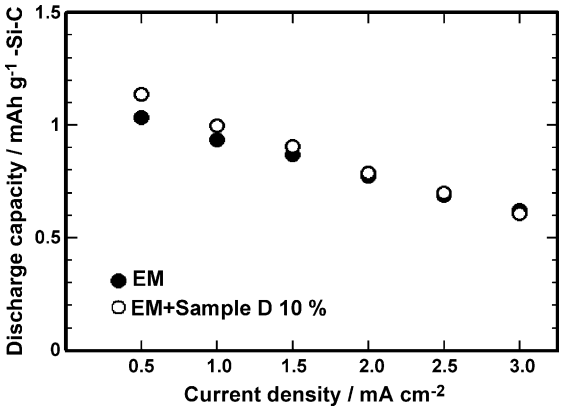

Fig. 20. Rate capability of Si–C/Li cells with EM + siloxane (sample D, 10 vol.%). Charge–discharge cut-off voltages, 0 and 1.5 V vs. Li/Li^+.

discharge capacity densities and the cycle life in EM + siloxanes were better than those in EM alone.

Fig. 20 shows the impedance of the interface between Si–C electrode and electrolyte solution. The impedance in EM + siloxane (sample D) was smaller than that in EM alone. Fig. 21 shows the discharge-rate capability of Si–C electrodes. The rate capability in EM + siloxanes was almost the same as that in EM alone. The discharge-rate determining step may be the lithium diffusion in the Si–C electrodes, not in the SEI.

From the charge–discharge cycling test results of lithium, Si–C and graphite electrodes, the effect of siloxane addition on charge–discharge cycling performance was obtained. However, there is a possibility that this effect arises from the improvement of cycling efficiency of lithium metal. Because all the cycling tests were carried out by using the coin cells with lithium metal electrodes. So, charge–discharge cycling tests of C/$LiCoO_2$ and Si–C/$LiCoO_2$ cells without lithium metal anodes were carried out.

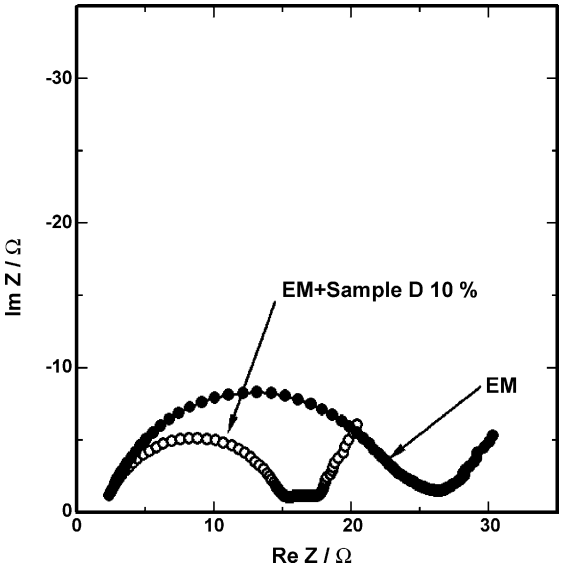

Fig. 21. Cole–Cole plot of Si–C(Li)/electrolyte interface, Si–C/Li cells after first charge, EM + sample D (10 vol.%) at 25 °C. Ips, 0.5 mA cm^{-2}; charge–discharge cut-off voltages, 0 and 1.5 V vs. Li/Li^+.

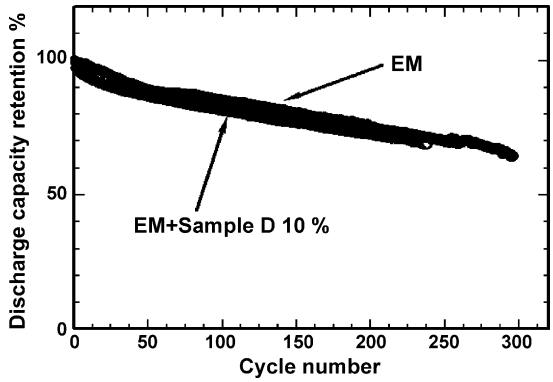

Fig. 22. Charge–discharge cycling tests results of graphite/$LiCoO_2$ cells with EM + siloxane (sample D, 10 vol.%). Ips, 0.5 mA cm^{-2}; charge–discharge cut-off voltages, 4.0 and 2.5 V.

3.4. Charge–discharge cycling properties of C/$LiCoO_2$ cells with siloxane electrolytes

Fig. 22 shows the charge–discharge cycling test results of graphite/$LiCoO_2$ cells. In Fig. 22, the discharge capacity at first cycle is defined as 100% retention. Almost the very similar cycling performance was obtained for both EM + siloxane (sample D) and EM alone. Fig. 23 shows the discharge capacity density based on $LiCoO_2$ weight. The capacity density in EM + siloxane was slightly larger than in EM alone. Fig. 24 shows the discharge capacity density based on graphite weight. The capacity density in EM + siloxane was considerably larger than in EM alone. Utilization of graphite anode improved by adding siloxane. So, by optimizing the charge–discharge cut-off voltages and the balance ratio of anode and cathode in the cell, the cycling performance may improve more.

3.5. Charge–discharge cycling properties of Si–C anode/$LiCoO_2$ cells with siloxane electrolytes

Fig. 25 shows the charge–discharge cycling test results of Si–C/$LiCoO_2$ cells. In Fig. 25, the discharge capacity at first cycle is defined as 100% retention. Slightly better cycling performance in EM + siloxane (sample D) than in EM alone was obtained. Fig. 26 shows the discharge capacity density

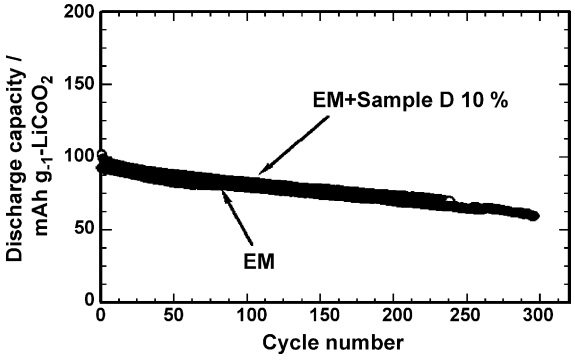

Fig. 23. Relationship between discharge capacity of $LiCoO_2$ and cycle number, graphite/LiCoO2 cells, EM + siloxane (sample D, 10 vol.%). Ips, 0.5 mA cm^{-2}; charge–discharge cut-off voltages, 4.0 and 2.5 V.

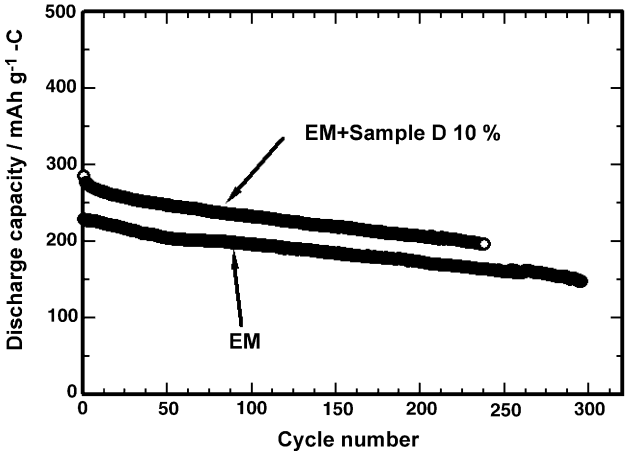

Fig. 24. Relationship between discharge capacity of graphite and cycle number, graphite/$LiCoO_2$ cells, EM + siloxane (sample D, 10 vol.%). Ips, 0.5 mA cm^{-2}; charge–discharge cut-off voltages, 4.0 and 2.5 V.

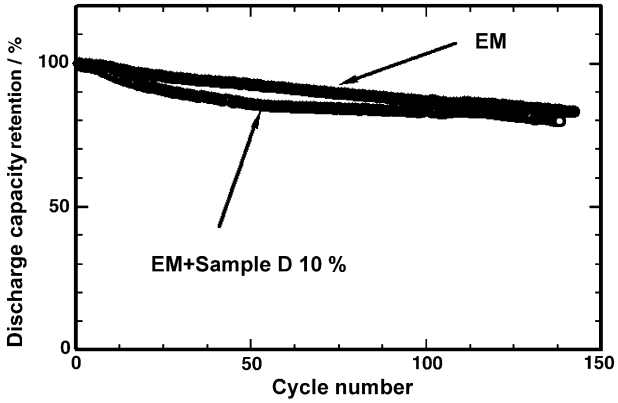

Fig. 25. Charge–discharge cycling test results of Si–C/$LiCoO_2$ cells with EM + siloxane (sample D, 10 vol.%). Ips, 0.5 mA cm^{-2}; charge–discharge cut-off voltages, 4.0 and 2.5 V.

based on $LiCoO_2$ weight. The capacity density of $LiCoO_2$ in EM + siloxane was slightly smaller than in EM alone. Fig. 27 shows the discharge capacity density based on Si–C weight. The capacity density of Si–C anodes in EM + siloxane was

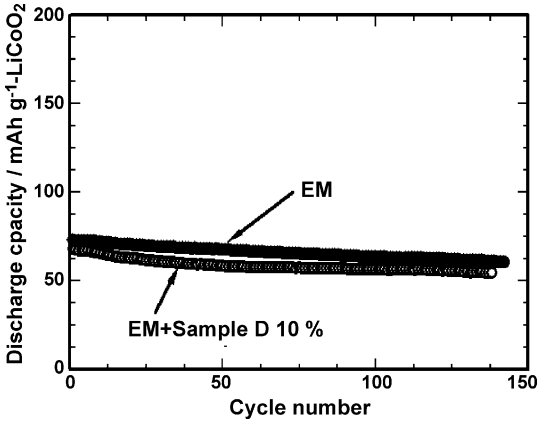

Fig. 26. Relationship between discharge capacity of $LiCoO_2$ and cycle number, Si–C/$LiCoO_2$ cells, EM + siloxane (sample D, 10 vol.%). Ips, 0.5 mA cm^{-2}; charge–discharge cut-off voltages, 4.0 and 2.5 V.

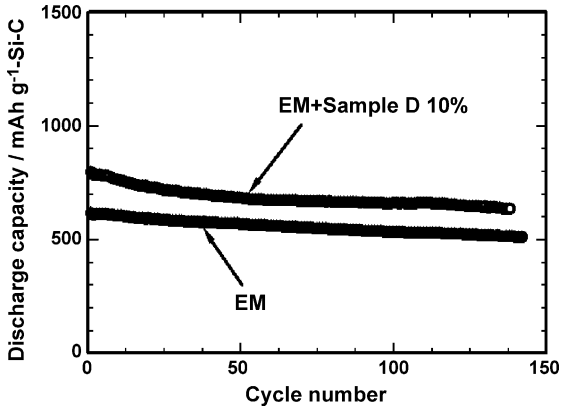

Fig. 27. Relationship between discharge capacity of Si–C and cycle number. Si–C/$LiCoO_2$ cells, EM + siloxane (sample D, 10 vol.%). Ips, 0.5 mA cm^{-2}; charge–discharge cut-off voltages, 4.0 and 2.5 V.

approximately 20% larger than in EM alone. Utilization of Si–C anode improved by adding siloxane. So, by optimizing the charge–discharge cut-off voltages and the balance ratio of anode and cathode in the cell, the cycling performance may improve more as in case of graphite anodes.

3.6. Thermal stability tests of electrolyte solutions with siloxanes

Thermal stability of the electrolytes is important for the cell safety [9,10]. Two kinds of DSC measurements were carried out. First is the thermal stability test of electrolyte itself. Second is the reaction behavior of electrolyte solutions and lithium. In the latter test, instead of lithium metal, graphite–lithium (C_6Li_x) was used.

Fig. 28 shows the thermal stability test results of electrolyte solutions. In EM alone, heat output corresponding to the thermal decomposition of electrolyte solution was observed at 220 °C. In EM + siloxane 10 vol.% (sample D), temperature starting the heat output shifted to higher temperature and amount of heat output decreased. With an increase in siloxane content, the heat output starting temperature shifted to more higher temperature and amount of heat output decreased more. So, the thermal stability of the EM improved by adding siloxanes.

Fig. 29 shows the DSC results for C_6Li_x with electrolytes. C_6Li_x was prepared by discharging Li/graphite coin cell to 0 V

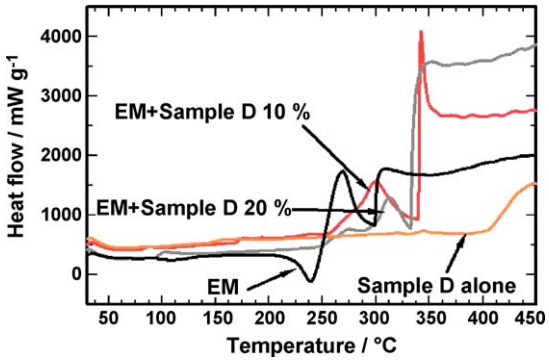

Fig. 28. DSC results of EM + siloxane (sample D). Scanning rate, 10 °C min^{-1}.

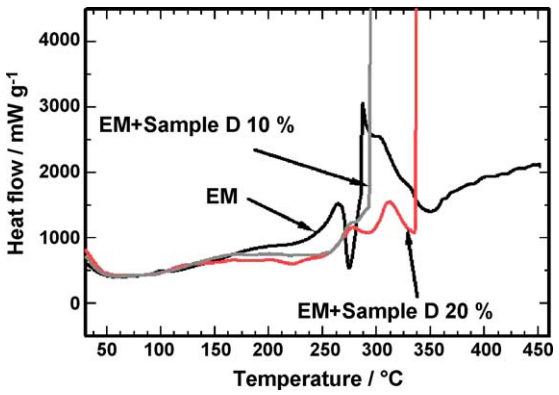

Fig. 29. DSC results of EM + siloxane (sample D) with $C_6Li_{0.97}$. Scanning rate, 10 °C min^{-1}.

at 0.5 mA cm^{-2}. The discharge product is $C_6Li_{0.97}$. In case of $C_6Li_{0.97}$ with EM alone, two heat generation regions were observed. The first heat output was mild and started at 130 °C. It continued until a sharp exothermic peak appeared at 280 °C. A possible mechanism for these DSC results is as follows [10]. The first mild heat output corresponded to the reduction of EM by the lithium inside the carbon. This reaction has already occurred at first charge and produced the SEI film on the carbon surface at room temperature. At 130 °C, the PVDF, electrode binder, swells. Then, the carbon that is not covered with SEI appears, and the lithium inside the carbon reacts with the electrolyte solution [10]. SEI is consisted of several chemical materials. Another possibility as the cause for first heat output is suggested to be the decomposition of the part of SEI compounds [11] or the conversion of metastable SEI components to stable SEI components [12]. At 280 °C, the surface SEI film is broken. Almost the whole of carbon surface appears, and the lithium in the carbon reacts vigorously with the electrolyte solution [10].

In case of $C_6Li_{0.97}$ with the EM + siloxanes, the amounts of heat out put decreased and the temperature starting heat output shifted to higher temperature. With an increase in siloxane content, this effect of siloxane on the improvement of the thermal stability of the EM toward $C_6Li_{0.97}$ became larger.

So, the addition of siloxane was effective on the suppression of both the thermal decomposition of the electrolyte solution and the reactivity of the electrolyte solution toward lithium. These effects of siloxanes may improve the cell safety. These results may arise from the difference of the SEI properties between EM alone and EM + siloxane as mentioned in Section 3.1.

4. Conclusion

Lithium cycling efficiencies of three kinds of anodes, lithium metal, graphite and Si–SiO_2–carbon composite (Si–C) anodes, improved by adding poly-ether modified siloxanes to EM. The impedance of anode/electrolyte interface decreased by adding siloxanes. Graphite/$LiCoO_2$ cells and Si–C/$LiCoO_2$ cells exhibited better anode utilization and good cycling performance by using EM + siloxane electrolytes. It was also

found that the thermal stability of the EM improved by adding siloxanes. The thermal decomposition temperature of the electrolyte solutions shifted to higher temperature by adding siloxanes. Amount of heat-output of graphite–lithium anodes with electrolyte solutions decreased and the temperature starting the heat-output shifted to higher temperature by adding siloxanes. By modifying chemical structure of siloxanes, more improvement of charge–discharge cycling performance of lithium cells should be obtained.

References

[1] N. Tamura, R. Ohshita, M. Fujimoto, M. Kamino, S. Fujitani, J. Electrochem. Soc. 150 (2003) A679.
[2] L.A. Dominey, in: G. Pistoia (Ed.), Lithium Batteries, Elsevier, The Netherlands, 1994 (chapter 4).
[3] M. Mori, Y. Narukawa, K. Naoi, D. Futeux, J. Electrochem. Soc. 145 (1998) 2340.
[4] M. Miyachi, H. Yamamoto, H. Kawai, T. Ohta, M. Shirakawa, Extended Abstracts of 206th Electrochemical Society Meeting, Abs. No. 311, 2004.
[5] T. Morita, N. Takami, Extended Abstracts of 206th Electrochemical Society Meeting, Abs. No. 312, 2004.
[6] Jpn. Kokai Tokkyo Koho (Jpn. patent application), JP2004-47404A, 2004.
[7] D. Aurbach, E. Granot, Electrochim. Acta 42 (1997) 697.
[8] E. Peled, D. Golodnitsky, J. Pencier, in: J.O. Besenhard (Ed.), Handbook of Battery Materials, Wiley-VCH, Germany, 1999 (chapter 6).
[9] S. Tobishima, J. Yamaki, J. Power Sources 81/82 (1999) 882.
[10] J. Yamaki, H. Takatsuji, T. Kawamura, M. Egashira, Solid State Ionics 148 (2002) 241.
[11] A. Du Pasquier, F. Disma, T. Bowmer, A.S. Gozdz, G. Amatucci, J.M. Tarascon, J. Electrochem. Soc. 145 (1998) 472.
[12] M.N. Richard, J.R. Dahn, J. Electrochem. Soc. 146 (1999) 2068.